

Variable Aerodynamic Damping via Co-Contraction: A Dynamic Isomorphism with Variable Stiffness Actuators

Antonio Franchi^{1,2}

Abstract—We prove that aerodynamic co-contraction in a redundant dual-rotor actuator can tune a passive, trim-defined aero-mechanical damping while keeping the commanded net force constant. In particular, we define an incremental damping coefficient as the local sensitivity of net thrust to air-relative velocity at a trim and prove that it increases monotonically along constant-force fibers under a mild aerodynamic hardening condition. We then validate the required damping and hardening properties from a first-principles Blade Element Theory derivation, which yields a minimal thrust model affine in inflow and explicitly reveals the speed–inflow coupling driving the effect. The resulting mechanism is formalized as a Variable Aerodynamic Damping Actuator (VADA) and shown to be dynamically isomorphic to stiffness modulation in antagonistic variable-stiffness actuation (VSA), similar to the co-contraction of tendons by muscle co-activation. The same fiber-density principle also enhances the active aerodynamic promptness measure of redundant multirotors. Finally, an impedance-form representation clarifies the roles of common-mode and differential-mode actuation in the control of passive impedance and the equilibrium velocity of the VADA system.

I. INTRODUCTION

Actuation redundancy is pervasive in multirotor aerial vehicles, including standard hexarotors/octorotors and fully actuated platforms [1, 2, 3], where multiple rotor-speed vectors can realize the same commanded wrench. This freedom is typically resolved by control-allocation strategies that minimize an effort proxy (least-norm or QP-type allocators), both in the control-allocation literature and in widely deployed flight stacks that implement effectiveness-matrix backends and constraint handling [4, 5] While such choices are well aligned with endurance, they do not explicitly optimize the *dynamic readiness* of the wrench response, which can become critical near weak-effectiveness regimes.

The ability to reject aggressive disturbances or execute agile maneuvers is limited not only by achievable steady-state wrench magnitudes, but also by the motor torque and rotor-acceleration constraints that bound *wrench-rate* generation [6, 7, 8, 9]. Motivated by the manipulability concept in robotics [10], the work of [11] introduced a geometric, fiber-based interpretation of this phenomenon for multirotors: moving along a constant-wrench fiber injects *internal* aerodynamic loading (aerodynamic co-contraction), thereby increasing the local fiber density and the associated

aerodynamic promptness (dynamic manipulability). However, in antagonistic Variable Stiffness Actuators (VSAs), co-contraction is known to play a dual role: it increases *active* authority while also shaping the *passive* mechanical response to external perturbations via impedance regulation [12, 13, 14, 15]. This observation raises a natural control question for redundant aerial actuation: *can aerodynamic co-contraction, while keeping the commanded wrench fixed, also tune a passive incremental input–output property of the vehicle?*

This work answers the above question in the affirmative, under a standard quasi-steady thrust model in which rotor thrust depends on both rotor speed and axial inflow [16]. Specifically, we formalize an *incremental aerodynamic damping* at a trim as the local map from air-relative velocity perturbations to aerodynamic force perturbations (a trim linearization coefficient), and show that traversing constant-force fibers through co-contraction monotonically increases this damping under a mild “aerodynamic hardening” condition. We verify this condition analytically via a first-order Blade Element Theory model and relate the resulting Variable Aerodynamic Damping Actuator (VADA) effect to the VSA stiffness mechanism through an explicit dynamic isomorphism.

Contributions. Compared to existing uses of manipulability in aerial robotics that focus on attached manipulators or static design indices [17, 18] and to the recent introduction of aerodynamic promptness [11], this work contributes with: (i) a trim-based definition of *aerodynamic damping modulation* enabled by redundancy and inflow coupling, (ii) a proof that co-contraction along constant-force fibers increases the damping coefficient under hardening, (iii) the introduction of the Variable Aerodynamic Damping Actuator (VADA) concept, and (iv) a compact impedance-form interpretation that clarifies the respective roles of common-mode and differential-mode actuation in the affine-inflow regime.

II. PASSIVE STIFFNESS AND ACTIVE PROMPTNESS IN ANTAGONISTIC VSAS

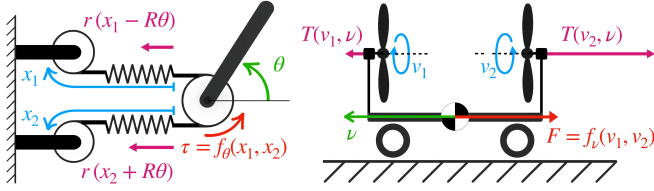
This section recalls a standard antagonistic Variable Stiffness Actuator (VSA) model [19] and makes explicit a basic but useful fact: along constant-torque fibers, internal co-contraction simultaneously increases (i) *passive* stiffness—the incremental torque response to external deflections—and (ii) *active* promptness—the local fiber density (manipulability) induced by the actuator task map, in the sense of [11]. Fig. 1a summarizes the variables and tendon routing.

Actuation model: Consider a single revolute joint with deflection $\theta \in \mathbb{R}$ driven by an antagonistic tendon mechanism.

¹Robotics and Mechatronics, Electrical Engineering, Mathematics, and Computer Science Faculty, University of Twente, The Netherlands.

²Department of Computer, Control and Management Engineering, Sapienza University of Rome, Rome, Italy. schol@r-franchi.eu

The work was partially funded by the European Commission Horizon Europe Framework under project Autoassess (101120732)



(a) Antagonistic VSA. Two motors generate joint torque and locally tune stiffness via co-contraction. (b) Antagonistic dual-rotor actuator (VADA). Two rotors generate net force and locally tune aerodynamic damping via co-contraction.

Fig. 1: Antagonistic actuation mechanisms. Both admit fiber motions corresponding to internal co-contraction: Variable Stiffness modulation in the VSA and Variable Aerodynamic Damping modulation in the dual-rotor actuator (VADA).

Let the actuator configuration be $\mathbf{x} = (x_1, x_2) \in \mathcal{X} \subset \mathbb{R}_{>0}^2$, where x_1, x_2 are motor-controlled tendon displacements, and let $R > 0$ be the pulley radius. The tendon force–extension law is modeled by a function $r : \mathbb{R} \rightarrow \mathbb{R}_{\geq 0}$.

Assumption II.1 (Strict hardening and local admissibility). *The tendon law satisfies $r \in \mathcal{C}^2$ and, for all $x > 0$, $r'(x) > 0$ and $r''(x) > 0$. We restrict attention to operating points and sufficiently small deflections such that $x_1 - R\theta > 0$ and $x_2 + R\theta > 0$ in the neighborhood of interest.*

Under this model, the net elastic torque exerted on the joint is $\tau : \mathcal{X} \times \mathbb{R} \rightarrow \mathbb{R}$ defined by

$$(\mathbf{x}, \theta) \mapsto \tau(\mathbf{x}, \theta) := R(r(x_1 - R\theta) - r(x_2 + R\theta)). \quad (1)$$

A. Stiffness and promptness at $\theta = 0$

At the nominal operating point $\theta = 0$, define the *task map* (active torque generation) $f : \mathcal{X} \rightarrow \mathbb{R}$ as

$$\mathbf{x} \mapsto f(\mathbf{x}) := \tau(\mathbf{x}, 0) = R(r(x_1) - r(x_2)). \quad (2)$$

The fiber of a desired torque $\bar{\tau} \in \mathbb{R}$ is the level set

$$\mathcal{F}_{\bar{\tau}} := f^{-1}(\bar{\tau}) = \{\mathbf{x} \in \mathcal{X} \mid f(\mathbf{x}) = \bar{\tau}\}, \quad (3)$$

consistent with the fiber viewpoint used in [11].

Passive stiffness: The *passive joint stiffness* $\sigma : \mathcal{X} \rightarrow \mathbb{R}_{>0}$ is the incremental resistance to external angular deflections at $\theta = 0$, defined by:

$$\mathbf{x} \mapsto \sigma(\mathbf{x}) := - \left. \frac{\partial \tau}{\partial \theta} \right|_{\theta=0} = R^2(r'(x_1) + r'(x_2)). \quad (4)$$

Active promptness (fiber density): The *active torque promptness* $\rho : \mathcal{X} \rightarrow \mathbb{R}_{\geq 0}$ is defined as the fiber-density (manipulability) under the Euclidean metric on actuator rates (see [11]) and is given by

$$\mathbf{x} \mapsto \rho(\mathbf{x}) := \sqrt{\det(J_f(\mathbf{x}) J_f^\top(\mathbf{x}))} \quad (5)$$

where $J_f(\mathbf{x}) := \nabla f(\mathbf{x})$. The scalar $\rho(\mathbf{x})$ quantifies the local sensitivity of the output torque to instantaneous changes in motor positions. For the scalar task (2), the Jacobian is

$$J_f(\mathbf{x}) = \nabla f(\mathbf{x}) = [R r'(x_1) \quad -R r'(x_2)], \quad (6)$$

which substituted in (5) gives

$$\rho(\mathbf{x}) = \|J_f(\mathbf{x})\| = R\sqrt{r'(x_1)^2 + r'(x_2)^2}. \quad (7)$$

Remark II.2 (Different physical roles). *Although both σ and ρ are induced by the same nonlinear map, they encode different incremental phenomena: σ maps external deflections to passive restoring torque ($\Delta\theta \mapsto \Delta\tau$), whereas ρ maps internal actuation variations to active torque changes ($\Delta\mathbf{x} \mapsto \Delta\tau$).*

B. Strict monotonic coupling along constant-torque fibers

Definition II.3 (Internal co-contraction direction). *Let $\mathbf{x} \in \mathcal{F}_{\bar{\tau}}$. A nonzero displacement $d\mathbf{x} = [dx_1, dx_2]^\top \in T_{\mathbf{x}}\mathcal{F}_{\bar{\tau}}$ is an internal co-contraction if $dx_1 > 0$ and $dx_2 > 0$.*

Proposition II.4 (Co-contraction increases stiffness and promptness). *Under Assumption II.1, along any constant-torque fiber $\mathcal{F}_{\bar{\tau}}$, every internal co-contraction displacement strictly increases both σ and ρ . Moreover, on any connected 1D branch of $\mathcal{F}_{\bar{\tau}}$, σ and ρ are strictly monotonically related.*

Proof. Let $\mathbf{x} \in \mathcal{F}_{\bar{\tau}}$ and $d\mathbf{x} \in T_{\mathbf{x}}\mathcal{F}_{\bar{\tau}}$. Differentiating (2) and enforcing $df = 0$ yields

$$0 = df = R(r'(x_1) dx_1 - Rr'(x_2) dx_2) \Rightarrow \frac{dx_2}{dx_1} = \frac{r'(x_1)}{r'(x_2)}. \quad (8)$$

Since $r'(x) > 0$ for $x > 0$, (8) implies that dx_1 and dx_2 have the same sign, hence co-contraction is an admissible fiber direction. From (4),

$$d\sigma = R^2(r''(x_1) dx_1 + r''(x_2) dx_2), \quad (9)$$

which is strictly positive under Assumption II.1 and $dx_1, dx_2 > 0$. Similarly, from (7) and $\rho > 0$,

$$d\rho = \frac{R}{\rho(\mathbf{x})} (r'(x_1)r''(x_1) dx_1 + r'(x_2)r''(x_2) dx_2), \quad (10)$$

which is strictly positive because $r'(x_i) > 0$, $r''(x_i) > 0$, and $dx_i > 0$. Hence both σ and ρ strictly increase along any \mathcal{C}^1 co-contraction parameterization $\mathbf{x}(s) \subset \mathcal{F}_{\bar{\tau}}$.

Finally, on any connected 1D fiber branch, strict monotonicity implies that $s \mapsto \sigma(\mathbf{x}(s))$ is invertible, and therefore ρ is a strictly increasing function of σ along that branch (equivalently, $d\rho/d\sigma > 0$). \square

Proposition II.4 formalizes that, for antagonistic mechanisms with strictly hardening elasticity, stiffness modulation through co-contraction is accompanied by a simultaneous and monotone increase of the local torque promptness (fiber density) along constant-torque fibers. This observation will serve as the mechanical reference point for the aerodynamic damping modulation developed in the next sections.

III. THE DUAL-ROTOR AERODYNAMIC ACTUATOR

We introduce a minimal redundant aerodynamic actuator that already exhibits an antagonistic internal mode. A rigid body is constrained to translate along a line and is actuated by two propellers whose thrust axes are collinear with the translation direction (Fig. 1b). Let $\nu \in \mathbb{R}$ denote the *air-relative* translational velocity along this axis (positive in the

forward direction; in still air it coincides with the body speed). The control inputs are the propeller angular speeds $\mathbf{v} = (v_1, v_2) \in \mathcal{V} \subset \mathbb{R}_{\geq 0}^2$. The propellers are mounted antagonistically so that rotor 1 contributes force in the $+\nu$ direction while rotor 2 contributes force in the $-\nu$ direction. As a result, for a given commanded net force there typically exists a one-dimensional family of speed pairs, enabling internal *co-contraction* (simultaneous increase of both speeds) as in antagonistic tendon actuation, see [11].

Non-interference (no rotor-rotor slipstream coupling): To isolate the operating-point dependence of each rotor on axial inflow, we assume negligible mutual wake interaction.

Assumption III.1 (Negligible mutual aerodynamic interference). *The rotors are mounted with sufficient separation and/or lateral offset such that, in the operating regime of interest, the inflow at each rotor disk is well approximated by the ambient axial inflow induced by the body's motion, and not by the other rotor's slipstream.*

Single-rotor thrust map: Let

$$T : \mathbb{R}_{\geq 0} \times \mathbb{R} \rightarrow \mathbb{R}_{\geq 0}, \quad (v, \nu_{in}) \mapsto T(v, \nu_{in})$$

denote the thrust magnitude generated by a single propeller at angular speed v under axial inflow velocity ν_{in} . We adopt the convention that $\nu_{in} > 0$ denotes inflow that reduces the effective angle of attack (advance-ratio convention), so that increasing ν_{in} tends to reduce thrust in the regime of interest. Under Assumption III.1 and the antagonistic mounting of Fig. 1b, the two rotors experience opposite inflows:

$$\nu_{in,1} = \nu, \quad \nu_{in,2} = -\nu. \quad (11)$$

Accordingly, the *net aerodynamic force* along the axis is

$$F(\mathbf{v}, \nu) = T(v_1, \nu) - T(v_2, -\nu). \quad (12)$$

Regularity and monotonicity properties: We will use the following local properties, which are standard under low-to-moderate advance-ratio operation and will be verified explicitly in Sec. V for a first-order Blade Element Theory model.

Assumption III.2 (Monotone thrust in rotor speed). *In the operating regime of interest, T is C^2 and $\frac{\partial T}{\partial v}(v, \nu_{in}) > 0$ for all $v > 0$.*

Assumption III.3 (Aerodynamic damping in inflow). *For any fixed $v > 0$, increasing axial inflow reduces thrust. Equivalently, the inflow-sensitivity*

$$\lambda(v, \nu_{in}) := -\frac{\partial T}{\partial \nu_{in}}(v, \nu_{in}) > 0 \quad (13)$$

holds in the operating regime.

Assumption III.4 (Aerodynamic ‘‘hardening’’ of damping). *The inflow-sensitivity increases with rotor speed, i.e.,*

$$\frac{\partial \lambda}{\partial v}(v, \nu_{in}) = -\frac{\partial^2 T}{\partial \nu_{in} \partial v}(v, \nu_{in}) > 0, \quad \forall v > 0. \quad (14)$$

Remark III.5 (Analogy with mechanical hardening). *Assumption III.4 mirrors Assumption II.1: $r''(x) > 0$ implies*

that incremental stiffness grows with internal displacement, whereas $-\partial^2 T / (\partial \nu_{in} \partial v) > 0$ implies that the incremental inflow sensitivity (and thus the local damping effect defined next) grows with internal rotor speed. Section V provides a first-principles verification under a simple thrust model.

IV. THE VARIABLE AERODYNAMIC DAMPING ACTUATOR (VADA)

We now formalize the passive dynamical quantity that, for the dual-rotor aerodynamic actuator, plays the same structural role that stiffness plays in antagonistic VSAs.

A. Incremental aerodynamic damping at $\nu = 0$

We define the *passive aerodynamic damping* as the incremental resistance of the net aerodynamic force to small perturbations of air-relative velocity, evaluated at $\nu = 0$:

$$\sigma_a(\mathbf{v}) := -\left. \frac{\partial F}{\partial \nu} \right|_{\nu=0}. \quad (15)$$

Using (12) and the chain rule with (11) yields

$$\begin{aligned} \sigma_a(\mathbf{v}) &= -\left[\frac{\partial T}{\partial \nu_{in}}(v_1, 0) \cdot 1 - \frac{\partial T}{\partial \nu_{in}}(v_2, 0) \cdot (-1) \right] \\ &= \lambda(v_1, 0) + \lambda(v_2, 0). \end{aligned} \quad (16)$$

Equation (16) is structurally identical to the VSA stiffness $\sigma(x) = R^2(r'(x_1) + r'(x_2))$ in (4), with $\lambda(\cdot, 0)$ replacing $r'(\cdot)$.

B. Aerodynamic co-contraction along constant-force fibers

At $\nu = 0$, define the *force task map* $f_a : \mathcal{V} \rightarrow \mathbb{R}$ by

$$f_a(\mathbf{v}) := F(\mathbf{v}, 0) = T(v_1, 0) - T(v_2, 0), \quad (17)$$

and let the fiber at a commanded force \bar{F} be

$$\mathcal{F}_{\bar{F}} := \{\mathbf{v} \in \mathcal{V} \mid f_a(\mathbf{v}) = \bar{F}\}. \quad (18)$$

Definition IV.1 (Aerodynamic internal co-contraction). *Let $\mathbf{v} \in \mathcal{F}_{\bar{F}}$. A nonzero displacement $d\mathbf{v} = [dv_1, dv_2]^\top \in T_{\mathbf{v}}\mathcal{F}_{\bar{F}}$ is an aerodynamic co-contraction direction if $dv_1 > 0$ and $dv_2 > 0$.*

Proposition IV.2 (Co-contraction increases aerodynamic damping). *Under Assumptions III.2 and III.4, along any constant-force fiber $\mathcal{F}_{\bar{F}}$, every aerodynamic co-contraction displacement strictly increases the passive aerodynamic damping σ_a .*

Proof. Along $\mathcal{F}_{\bar{F}}$ we have $df_a = 0$. Differentiating (17) gives

$$0 = df_a = \frac{\partial T}{\partial v}(v_1, 0) dv_1 - \frac{\partial T}{\partial v}(v_2, 0) dv_2, \quad (19)$$

hence

$$\frac{dv_2}{dv_1} = \frac{\frac{\partial T}{\partial v}(v_1, 0)}{\frac{\partial T}{\partial v}(v_2, 0)}. \quad (20)$$

By Assumption III.2, the numerator and denominator are positive for $v_1, v_2 > 0$, hence dv_1 and dv_2 share the same sign and co-contraction is an admissible fiber direction.

From (16), the differential of σ_a is

$$d\sigma_a = \frac{\partial \lambda}{\partial v}(v_1, 0) dv_1 + \frac{\partial \lambda}{\partial v}(v_2, 0) dv_2. \quad (21)$$

Assumption III.4 yields $\partial \lambda / \partial v > 0$, and co-contraction implies $dv_1, dv_2 > 0$, hence $d\sigma_a > 0$. \square

C. Active aerodynamic promptness (fiber density)

A complementary *active* quantity is the local fiber density (promptness), which measures how effectively bounded rotor-speed variations can generate force-rate variations [11]. For the scalar task map (17), the Jacobian is

$$J_{f_a}(v) = \nabla f_a(\mathbf{v}) = \left[\frac{\partial T}{\partial v}(v_1, 0) \quad -\frac{\partial T}{\partial v}(v_2, 0) \right], \quad (22)$$

and, under the Euclidean metric on actuator rates, the promptness scalar reduces to

$$\rho_a(v) := \sqrt{\det(J_{f_a} J_{f_a}^\top)} = \|J_{f_a}(v)\| = \sqrt{\left(\frac{\partial T}{\partial v}(v_1, 0)\right)^2 + \left(\frac{\partial T}{\partial v}(v_2, 0)\right)^2}. \quad (23)$$

For the quadratic static thrust law $T(v_i, 0) = k_T v_i^2$ used in [11], (23) yields $\rho_a(v) = 2k_T \sqrt{v_1^2 + v_2^2}$, recovering the same ‘‘promptness increases with co-contraction’’ effect in antagonistic regimes which was first shown in [11].

D. Definition of VADA and dynamic isomorphism

Definition IV.3 (Variable Aerodynamic Damping Actuator (VADA)). *The dual-rotor aerodynamic actuator (12) is a Variable Aerodynamic Damping Actuator if there exists a family of constant-force fibers $\{\mathcal{F}_{\bar{F}}\}$ on which internal co-contraction (Def. IV.1) can strictly increase the passive aerodynamic damping σ_a in (15).*

Remark IV.4 (Dynamic isomorphism with antagonistic VSAs). *Definition IV.3 and Proposition IV.2 are the dynamical counterparts of Proposition II.4 for antagonistic VSAs. The correspondence follows from the formal replacements*

$$(\mathbf{x}, r', r'') \longleftrightarrow (\mathbf{v}, \lambda(\cdot, 0), \partial\lambda/\partial v(\cdot, 0)),$$

together with the interpretation that v is the VADA’s environmental velocity perturbation dual to the VSA’s environmental deflection θ . Under this mapping, co-contraction modulates passive stiffness in VSAs and passive aerodynamic damping in the dual-rotor actuator; while simultaneously increasing the active promptness (fiber density) in both systems.

V. VALIDATION VIA BLADE ELEMENT THEORY

This section validates Assumptions III.3–III.4 by exhibiting a minimal thrust expression derived from a first-order Blade Element Theory (BET) argument [20]. The purpose is not high-fidelity rotorcraft modeling, but to make explicit, in closed form, the mixed speed–inflow coupling that underlies the proposed ‘‘aerodynamic hardening’’ mechanism, in direct analogy with mechanical hardening in Sec. II.

A. A first-order thrust model affine in inflow

To avoid notational overload, we consider a *single* propeller and denote its angular speed by $v > 0$. Let $\nu_{in} \in \mathbb{R}$ denote the axial inflow velocity at the rotor disk, with the sign convention of Sec. III (positive ν_{in} reduces thrust in the regime of interest). Consider a propeller with N blades of radius B , constant chord c , and constant pitch angle θ_0 . For a blade element at radius $b \in [0, B]$, the tangential speed is $\nu_T = vb$. Under a small-angle, first-order approximation and

neglecting induced inflow and profile-drag corrections, the inflow angle satisfies

$$\phi(b) \approx \frac{\nu_{in}}{vr}, \quad (24)$$

so that the effective angle of attack is

$$\alpha(b) \approx \theta_0 - \phi(b) \approx \theta_0 - \frac{\nu_{in}}{vr}. \quad (25)$$

Assuming a linear lift regime $C_L = a\alpha$ with lift-curve slope $a > 0$, the elemental thrust produced by the blade section of width db is approximated as

$$\begin{aligned} dT &\approx \frac{1}{2} N \rho_a c C_L \nu_T^2 dr = \frac{1}{2} N \rho_a c a \left(\theta_0 - \frac{\nu_{in}}{vb} \right) (vb)^2 dr \\ &= \frac{1}{2} N \rho_a c a (\theta_0 b^2 v^2 - vb \nu_{in}) dr. \end{aligned} \quad (26)$$

where ρ_a is the air density. Integrating over $b \in [0, B]$ yields

$$T(v, \nu_{in}) = \frac{1}{2} N \rho_a c a \left(\frac{\theta_0 B^3}{3} v^2 - \frac{B^2}{2} v \nu_{in} \right). \quad (27)$$

Defining the positive constants

$$k_T := \frac{1}{6} N \rho_a c a \theta_0 B^3 > 0, \quad k_D := \frac{1}{4} N \rho_a c a B^2 > 0, \quad (28)$$

we obtain the canonical first-order *affine-inflow* thrust model

$$T(v, \nu_{in}) = k_T v^2 - k_D v \nu_{in}. \quad (29)$$

B. Verification of damping and hardening

Proposition V.1 (Verification of aerodynamic damping). *For (29), the inflow-sensitivity $\lambda(v, \nu_{in}) := -\partial T/\partial \nu_{in}$ satisfies $\lambda(v, \nu_{in}) > 0$ for all $v > 0$.*

Proof. From (29), $\lambda(v, \nu_{in}) = -\frac{\partial T}{\partial \nu_{in}} = k_D v$, which is strictly positive for $v > 0$ since $k_D > 0$. \square

Proposition V.2 (Verification of aerodynamic hardening). *For (29), the inflow-sensitivity is strictly increasing in rotor speed: $\frac{\partial \lambda}{\partial v}(v, \nu_{in}) > 0$ for all $v > 0$.*

Proof. Using $\lambda(v, \nu_{in}) = k_D v$ gives $\frac{\partial \lambda}{\partial v} = k_D > 0$. \square

Remark V.3 (Consistency with monotone thrust in rotor speed). *Model (29) yields $\frac{\partial T}{\partial v} = 2k_T v - k_D \nu_{in}$. Hence $\partial T/\partial v > 0$ holds at least locally around $\nu_{in} = 0$ for any $v > 0$, and more generally whenever $\nu_{in} < 2(k_T/k_D)v$. This supports Assumption III.2 in the operating regime used in Sec. IV.*

C. A minimal ‘‘quadratic spring’’ analogue

The mixed term $-k_D v \nu_{in}$ in (29) is precisely the ingredient that enables VADA behavior. It implies $\lambda(v, \nu_{in}) = k_D v$, i.e., the incremental inflow sensitivity (and thus the incremental damping defined in Sec. IV) grows linearly with the internal actuation level v . This is directly analogous to an antagonistic VSA with quadratic hardening $r(x) = \frac{1}{2} k x^2$, for which the incremental stiffness is $r'(x) = kx$ and grows linearly with internal displacement. Accordingly, within the validity of the first-order model, aerodynamic co-contraction provides a principled mechanism to tune an effective aerodynamic damping around a trim, thereby fully complementing the kinematic ‘‘Flying Muscle’’ viewpoint of [11].

VI. GENERALIZATION TO A GENERIC TRIM AIRSPEED

Sections III–IV specialized the definitions to $\nu = 0$, which is the natural analogue of the VSA equilibrium $\theta = 0$. The same incremental notion of aerodynamic damping, however, is defined at any trim airspeed $\bar{\nu} \in \mathbb{R}$ and can be modulated along the corresponding constant-force fibers.

A. Incremental damping around $\nu = \bar{\nu}$

Recall the net force map $F(\mathbf{v}, \nu) = T(v_1, \nu) - T(v_2, -\nu)$, with $\mathbf{v} = (v_1, v_2) \in \mathcal{V} \subset \mathbb{R}_{>0}^2$. For a fixed operating point \mathbf{v} and trim airspeed $\bar{\nu}$, define the *incremental aerodynamic damping* as

$$\sigma_a(\mathbf{v}; \bar{\nu}) := - \left. \frac{\partial F}{\partial \nu} \right|_{\nu=\bar{\nu}}. \quad (30)$$

Using the chain rule and $\lambda(v, \nu_{in}) := -\partial T / \partial \nu_{in}$ yields

$$\sigma_a(\mathbf{v}; \bar{\nu}) = \lambda(v_1, \bar{\nu}) + \lambda(v_2, -\bar{\nu}). \quad (31)$$

Under Assumption III.3, $\sigma_a(\mathbf{v}; \bar{\nu}) > 0$ in the operating regime of interest. This is the direct trim analogue of the VSA stiffness $\sigma(\mathbf{x})$ defined at $\theta = 0$ in (4).

B. Co-contraction on constant-force fibers at $\nu = \bar{\nu}$

Fix a desired net force \bar{F} at the trim $\bar{\nu}$, and define the corresponding *trim task map* $f_{a, \bar{\nu}} : \mathcal{V} \rightarrow \mathbb{R}$ by

$$f_{a, \bar{\nu}}(\mathbf{v}) := F(\mathbf{v}, \bar{\nu}) = T(v_1, \bar{\nu}) - T(v_2, -\bar{\nu}), \quad (32)$$

The associated fiber is the level set

$$\mathcal{F}_{\bar{F}}^{\bar{\nu}} := \{ \mathbf{v} \in \mathcal{V} \mid f_{a, \bar{\nu}}(\mathbf{v}) = \bar{F} \}. \quad (33)$$

Proposition VI.1 (Co-contraction increases incremental damping at a trim). *Assume that T is \mathcal{C}^2 and that Assumptions III.2 and III.4 hold at inflows $\nu_{in} \in \{\bar{\nu}, -\bar{\nu}\}$. Then, along any constant-force fiber $\mathcal{F}_{\bar{F}}^{\bar{\nu}}$, every aerodynamic co-contraction displacement (Def. IV.1) strictly increases $\sigma_a(\cdot; \bar{\nu})$.*

Proof. On $\mathcal{F}_{\bar{F}}^{\bar{\nu}}$ we have $df_{a, \bar{\nu}} = 0$. Differentiating $f_{a, \bar{\nu}}(\mathbf{v}) = T(v_1, \bar{\nu}) - T(v_2, -\bar{\nu})$ gives

$$0 = \frac{\partial T}{\partial v}(v_1, \bar{\nu}) dv_1 - \frac{\partial T}{\partial v}(v_2, -\bar{\nu}) dv_2. \quad (34)$$

By Assumption III.2, both partial derivatives are positive for $v_1, v_2 > 0$, hence dv_1 and dv_2 share the same sign; in particular, $dv_1, dv_2 > 0$ is an admissible fiber direction.

From (31),

$$d\sigma_a = \frac{\partial \lambda}{\partial v}(v_1, \bar{\nu}) dv_1 + \frac{\partial \lambda}{\partial v}(v_2, -\bar{\nu}) dv_2. \quad (35)$$

Assumption III.4 implies $\partial \lambda / \partial v > 0$ at $\nu_{in} \in \{\bar{\nu}, -\bar{\nu}\}$, and co-contraction implies $dv_1, dv_2 > 0$, hence $d\sigma_a > 0$. \square

Remark VI.2 (Wind and air-relative speed). *If the body speed is v_{body} and the wind speed along the axis is v_{wind} , then $\nu = v_{\text{body}} - v_{\text{wind}}$. The above trim formulation therefore applies under steady wind by selecting $\bar{\nu} = \bar{v}_{\text{body}} - v_{\text{wind}}$.*

VII. AERODYNAMIC IMPEDANCE AND PASSIVE VELOCITY CONTROL WITH VARIABLE DAMPING

The physical meaning of the incremental damping becomes transparent by embedding the force map into the translational dynamics. Assume still air, let $m > 0$ be the body mass, $\nu \in \mathbb{R}$ the air-relative velocity, and F_{ext} an external disturbance force along the axis. The dynamics read

$$m\dot{\nu} = F(\mathbf{v}, \nu) + F_{\text{ext}}, \quad (36)$$

with $F(\mathbf{v}, \nu)$ given by (12).

A. Impedance structure under the affine-inflow thrust model

Consider the affine-inflow thrust model of Sec. V. Plug (29) with $k_T > 0$ and $k_D > 0$, in (12) using $\nu_{in,1} = \nu$ and $\nu_{in,2} = -\nu$ and then in (36) thus obtaining

$$m\dot{\nu} = k_T(v_1^2 - v_2^2) - k_D(v_1 + v_2)\nu + F_{\text{ext}}. \quad (37)$$

Rearranging highlights an impedance-like form,

$$m\dot{\nu} + c_{\text{app}}(\mathbf{v})\nu = F_{\text{act}}(\mathbf{v}) + F_{\text{ext}}, \quad (38)$$

where

$$c_{\text{app}}(\mathbf{v}) := k_D(v_1 + v_2), \quad F_{\text{act}}(\mathbf{v}) := k_T(v_1^2 - v_2^2). \quad (39)$$

The coefficient $c_{\text{app}}(\mathbf{v})$ is a physical viscous term: it multiplies the air-relative velocity and thus represents a resistive force that an external agent would experience when perturbing the motion. Moreover, for (29) one has $\lambda(v, 0) = k_D v$, so $c_{\text{app}}(\mathbf{v}) = \sigma_a(\mathbf{v})$ as defined in (16).

B. Equilibrium velocity and common-/differential-mode roles

Set $F_{\text{ext}} = 0$ and consider constant rotor speeds. An equilibrium velocity ν_{eq} satisfies $\dot{\nu} = 0$ in (37), i.e.,

$$k_D(v_1 + v_2)\nu_{\text{eq}} = k_T(v_1^2 - v_2^2) = k_T(v_1 - v_2)(v_1 + v_2). \quad (40)$$

Provided $v_1 + v_2 > 0$, this yields

$$\nu_{\text{eq}}(\mathbf{v}) = \frac{k_T}{k_D}(v_1 - v_2). \quad (41)$$

Using (39)–(41), (38) can be rewritten as

$$m\dot{\nu} + c_{\text{app}}(\mathbf{v})(\nu - \nu_{\text{eq}}(\mathbf{v})) = F_{\text{ext}}, \quad (42)$$

since $F_{\text{act}}(\mathbf{v}) = c_{\text{app}}(\mathbf{v})\nu_{\text{eq}}(\mathbf{v})$ under (29).

Equation (42) exposes a VSA-like separation of roles in this affine-inflow regime: the *differential* component $(v_1 - v_2)$ sets the equilibrium air-relative velocity, while the *common-mode* component $(v_1 + v_2)$ sets the passive damping c_{app} and thus the rate of rejection of velocity perturbations. Accordingly, aerodynamic co-contraction provides a direct knob to tune a passive velocity impedance around the trim while leaving the commanded equilibrium velocity to the differential actuation component.

VIII. DISCUSSION AND CRITICAL ANALYSIS

The preceding sections establish a precise sense in which antagonistic mechanical VSAs and redundant aerodynamic actuation (VADA) share a common geometric mechanism—motions along task fibers that implement internal co-contraction—while differing in the *order* of the environmental perturbation to which the passive response applies.

Disturbance order and impedance type: In an antagonistic VSA, the relevant environmental perturbation is a small *displacement* of the joint coordinate (here, $\theta \in \mathbb{R}$), and co-contraction modulates the incremental map $\Delta\theta \mapsto \Delta\tau$, i.e., stiffness (Sec. II). In the dual-rotor VADA, the relevant environmental perturbation is a small *air-relative velocity* (here, $\nu \in \mathbb{R}$), and co-contraction modulates the incremental map $\Delta\nu \mapsto \Delta F$, i.e., aerodynamic damping (Secs. IV–VII).

Why damping (and not stiffness) is the natural aerodynamic analogue: Under quasi-steady aerodynamic models, the instantaneous aerodynamic wrench depends on local flow conditions (including air-relative velocity) rather than on absolute position. Accordingly, the passive term emerging in a trim linearization is viscous-like and is naturally quantified by $-\partial F/\partial\nu$ (or, in higher dimension, by the symmetric part of the incremental velocity-to-wrench map at a trim). In this sense, navigating the nonlinear null-space (co-contraction along constant-force fibers) does not create a position-dependent restoring force; instead, it increases the local velocity coupling, effectively “thickening” the surrounding fluid in the incremental input–output behavior.

Energetic cost and promptness: The VADA perspective complements the kinematic “Flying Muscle” view of [11] by adding a dynamical interpretation: the same internal loading that increases active aerodynamic promptness (fiber density) can also increase passive aerodynamic damping. This suggests a unified viewpoint for redundant multirotor allocation as a geometry-aware regulation of both *active* authority and *passive* impedance, traded against energetic cost, with the dual-rotor case serving as the simplest setting where these mechanisms can be isolated and stated explicitly.

IX. CONCLUSION AND FUTURE WORK

This work introduced the *Variable Aerodynamic Damping Actuator (VADA)* viewpoint: for a redundant aerodynamic actuator whose thrust depends on axial inflow, co-contraction along constant-force fibers can monotonically increase an incremental (trim-defined) aerodynamic damping. A first-order Blade Element Theory model was used to verify the required aerodynamic hardening” property in closed form, and an impedance representation clarified the respective roles of common-mode and differential-mode actuation.

Future work will pursue two directions. First, experimental identification on a minimal dual-rotor setup would quantify the magnitude of the damping modulation and its energetic cost, complementing the present analytical evidence. Second, extending the analysis to more general multirotor geometries and coupled inflow effects is of interest: while the basic VADA mechanism is expected to persist whenever inflow-dependent thrust and redundancy coexist, its manifestation may be intertwined with additional aerodynamic and structural couplings. In this respect, the present minimal configuration is intended as a deliberate abstraction that exposes the core principle before addressing more complex platforms.

REFERENCES

- [1] S. Park, J. Lee, J. Ahn, M. Kim, J. Her, G.-H. Yang, and D. Lee. “ODAR: Aerial Manipulation Platform Enabling Omnidirectional Wrench Generation”. In: *IEEE/ASME Trans. on Mechatronics* 23.4 (2018), pp. 1907–1918.
- [2] K. Bodie, Z. Taylor, M. Kamel, and R. Siegwart. “Towards Efficient Full Pose Omnidirectionality with Overactuated MAVs”. In: *Proc. of the 2018 Int. Symposium on Experimental Robotics (ISER)*. Springer, 2020, pp. 85–95.
- [3] M. Ryll, H. H. Bühlhoff, and P. Robuffo Giordano. “A Novel Overactuated Quadrotor UAV: Modeling, Control and Experimental Validation”. In: *IEEE Trans. on Control Systems Technology* 23.2 (2015), pp. 540–556.
- [4] M. Bodson. “Evaluation of Optimization Methods for Control Allocation”. In: *Journal of Guidance, Control, and Dynamics* 25.4 (2002), pp. 703–711.
- [5] D. Brescianini and R. D’Andrea. “Design, Modeling and Control of an Omni-Directional Aerial Vehicle”. In: *Proc. of the IEEE Int. Conf. on Robotics and Automation (ICRA)*. Stockholm, Sweden, 2016, pp. 3261–3266.
- [6] A. Romero, S. Sun, P. Foehn, and D. Scaramuzza. “Model Predictive Contouring Control for Time-Optimal Quadrotor Flight”. In: *IEEE Trans. on Robotics* (2022). arXiv:2108.13205.
- [7] E. Kaufmann, A. Loquercio, R. Ranfil, M. Müller, V. Koltun, and D. Scaramuzza. “Deep Drone Acrobatics”. In: *Robotics: Science and Systems (RSS)*, 2020.
- [8] A. Saviolo, G. Li, and G. Loianno. “Physics-Inspired Temporal Learning of Quadrotor Dynamics for Accurate Model Predictive Trajectory Tracking”. In: *IEEE Robotics and Automation Letters* 7.3 (2022), pp. 7809–7816.
- [9] D. Bicego, J. Mazzetto, R. Carli, M. Farina, and A. Franchi. “Nonlinear Model Predictive Control with Enhanced Actuator Model for Multi-Rotor Aerial Vehicles with Generic Designs”. In: *Journal of Intelligent & Robotic Systems* 100.3–4 (2020), pp. 1213–1247.
- [10] T. Yoshikawa. “Manipulability of Robotic Mechanisms”. In: *The Int. Journal of Robotics Research* 4.2 (1985), pp. 3–9.
- [11] A. Franchi. “Muscle Coactivation in the Sky: Geometry and Pareto Optimality of Energy vs. Aerodynamic Promptness and Multirotors as Variable Stiffness Actuators”. In: *2026 Int. Conf. on Unmanned Aircraft Systems*. Corfu, Greece, June 2026, <https://arxiv.org/abs/2602.14222>.
- [12] N. Hogan. “Impedance Control: An Approach to Manipulation”. In: *Proc. of the American Control Conf (ACC)*. 1984, pp. 304–313.
- [13] E. Burdet, R. Osu, D. W. Franklin, T. E. Milner, and M. Kawato. “The Central Nervous System Stabilizes Unstable Dynamics by Learning Optimal Impedance”. In: *Nature* 414.6862 (2001), pp. 446–449.
- [14] D. W. Franklin, R. Osu, E. Burdet, M. Kawato, and T. E. Milner. “Adaptation to Stable and Unstable Dynamics Achieved by Combined Impedance Control and Inverse Dynamics Model”. In: *Journal of Neurophysiology* 90.5 (2003), pp. 3270–3282.
- [15] P. L. Gribble, L. I. Mullin, N. Cothros, and A. Mattar. “Role of Cocontraction in Arm Movement Accuracy”. In: *Journal of Neurophysiology* 89.5 (2003), pp. 2396–2405.
- [16] P.-J. Bristeau, P. Martin, E. Salaün, and N. Petit. “The Role of Propeller Aerodynamics in the Model of a Quadrotor UAV”. In: *European Control Conf (ECC)*. 2009, pp. 3550–3555.
- [17] F. Ruggiero, V. Lippiello, and A. Ollero. “Aerial Manipulation: A Literature Review”. In: *IEEE Robotics and Automation Letters* 3.3 (2018), pp. 1957–1964.
- [18] M. Hamandi, F. Usai, Q. Sablé, N. Staub, M. Tognon, and A. Franchi. “Design of Multirotor Aerial Vehicles: A Taxonomy Based on Input Allocation”. In: *The Int. Journal of Robotics Research* 40.8-9 (2021), pp. 1015–1044.
- [19] S. Wolf, G. Grioli, O. Eiberger, W. Friedl, M. Grebenstein, H. Höppner, E. Burdet, D. G. Caldwell, R. Carloni, M. G. Catalano, D. Lefeber, S. Stramigioli, N. Tsagarakis, M. Van Damme, R. Van Ham, B. Vanderborght, L. C. Visser, A. Bicchi, and A. Albu-Schäffer. “Variable Stiffness Actuators: Review on Design and Components”. In: *IEEE/ASME Trans. on Mechatronics* 21.5 (2016), pp. 2418–2430.
- [20] P. Volodin. *Blade Element Rotor Theory*. 1st ed. Boca Raton: CRC Press, 2022.